Macromolecules

ARTICLE

pubs.acs.org/Macromolecules

Graphite Oxide as a Dehydrative Polymerization Catalyst: A One-Step Synthesis of Carbon-Reinforced Poly(phenylene methylene) Composites

Daniel R. Dreyer,[†] Karalee A. Jarvis,[‡] Paulo J. Ferreira,[‡] and Christopher W. Bielawski*[,†]

[†]Department of Chemistry and Biochemistry, The University of Texas at Austin, 1 University Station, A1590, Austin, Texas 78712, United States

[‡]Materials Science and Engineering Program, The University of Texas at Austin, 1 University Station, C2200, Austin, Texas 78712, United States

Supporting Information

ABSTRACT: The synthesis and characterization of poly(phenylene methylene) (PPM) and carbon composites thereof are described. The materials were prepared using graphite oxide (GO), which was discovered to function in two distinct roles. First, the GO was found to facilitate the dehydrative polymerization of benzyl alcohol (BnOH) to form PPM. Second, the residual carbon from the GO catalyst, having undergone thermal deoxygenation during the polymerization reaction, served as a graphene-like additive in the resulting composite. While pure (i.e., additive-free) PPM was found to be mechanically compliant (E' = 40 MPa), inclusion of 0.1 wt % GO in the starting reaction mixture improved the material's mechanical properties significantly (E' = 320 MPa). Homogeneous dispersion of the additive in the matrix was confirmed by powder X-ray diffraction (PXRD) analysis, Raman spectroscopy, and transmission electron microscopy (TEM). The carbon additive was separated from the PPM via trituration in dichloromethane, and the GO starting material (C:O ratio = 2.0:1; $\sigma = 4.45 \times 10^{-5}$ S m^{-1}) was found to have undergone significant reduction during the polymerization reaction (C:O ratio = 12.3:1; σ = 801 S m^{-1}). Moreover, the recovered carbon did not assemble into graphite-like aggregates, as determined by PXRD, Raman spectroscopy, and TEM, which indicated that the PPM matrix was able to effectively disperse the additive.

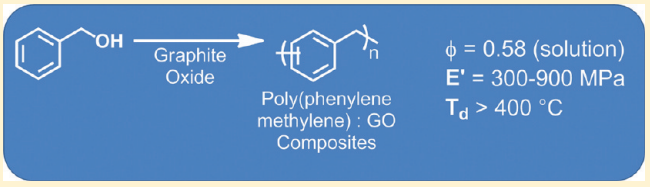

Polymer nanocomposites containing graphene or other similar carbon additives have found widespread utility, primarily due to the low loadings necessary to achieve significant enhancement in the targeted properties (e.g., mechanical, thermal, electronic, barrier, etc.).[1] However, the incorporation of metastable additives such as graphene is often challenged by their propensity to aggregate and phase separate from the polymer matrix.[2] From a processing perspective, the additive and matrix are typically combined via melt blending, extrusion, or other postpolymerization methods,[3−5] or through the *in situ* polymerization of a monomer in the presence of the carbon additive.[6,7] The latter of these approaches is generally more efficient as it minimizes or eliminates the need for extensive processing to ensure homogeneous dispersion of the additive in a preformed polymer.[8−10] *In situ* polymerizations are also preferred when interactions (either covalent or noncovalent) between an additive and its polymer matrix help stabilize the composite or provide enhanced mechanical, thermal, or electronic properties.[11−13] However, many of these *in situ* methods either require modification of the additive to ensure compatibility with the matrix or are not broadly applicable. Thus, simpler and more general *in situ* polymerization approaches are of high value. Toward this end, we envisioned exploiting the inherent catalytic properties of functionalized carbon materials as a means to facilitate the polymerization of various monomers. Given its high degree of functionality and demonstrated chemical reactivity,[14] we began by exploring the utility of graphite oxide (GO) in such roles.

Recently, we have shown that GO,[14,16−19] a carbon nanomaterial obtained in one step from inexpensive, commercially available starting materials (see Figure 1), is capable of facilitating a broad range of synthetic transformations.[20−23] The selective conversion of alcohols to aldehydes, alkynes to methyl ketones, and olefins to diones,[20] as well as various C−H oxidations[22] and autotandem combinations of these reactions,[21] have all been accomplished using this single, metal-free carbocatalyst.[24] As an extension of these chemistries and to address the issues discussed above, we have launched a program aimed at using GO as a catalyst for preparing a broad range of polymeric materials. In addition to facilitating valuable polymerizations, the use of a carbon as the reaction catalyst was expected to afford carbon-filled composites as the products and proceed without the need for postpolymerization incorporation of an additional additive (Figure 2).[25] Such an approach could potentially offer a significant improvement, with potentially broad applicability, over other methods for forming composites containing carbon additives such as graphene. The direct use of a carbon material as both the polymerization catalyst and additive condenses the process of

Received: June 9, 2011
Revised: July 26, 2011
Published: September 16, 2011

ACS Publications © 2011 American Chemical Society

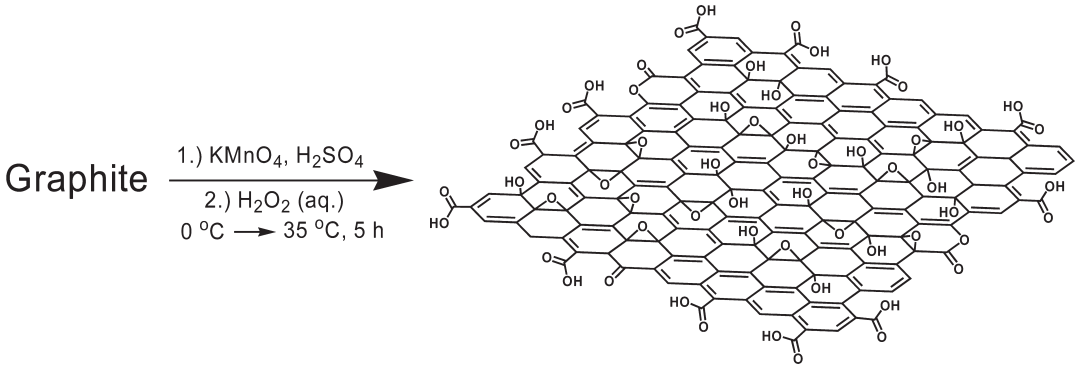

Figure 1. Synthesis and structure of graphite oxide (GO) according to the Lerf–Klinowski model.[14,15]

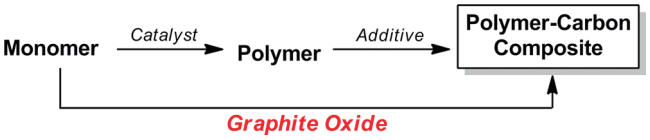

Figure 2. Comparison of approaches used to access carbon-filled composites. The conventional stepwise method is effectively circumvented through the use of graphite oxide (GO) as both the polymerization catalyst and the composite additive. The use of GO as the polymerization catalyst facilitates polymer formation as well as the formation of a product that is enhanced by graphene's remarkable chemical and physical properties.

composite formation to one facile step that requires no purification or further processing of the desired product. Herein we demonstrate this concept by showing that GO not only catalyzes the dehydrative polymerization of benzyl alcohol (BnOH), resulting in the formation of poly(phenylene methylene) (PPM), but also that mechanically robust PPM-based nanocomposites are formed in a single step.

PPM, also known as "polybenzyl",[26,27] is one of the oldest known polymers that belong to the poly(phenylene alkylene) class.[28] For example, Cannizzaro, Friedel, and Crafts each obtained an amorphous hydrocarbon consistent with the structure of $(C_7H_6)_n$ upon adding strong Lewis or Brønsted acids (e.g., BF_3, H_2SO_4, P_2O_5, or $AlCl_3$) to benzyl halides or benzyl alcohol.[26,29−33] Since those early experiments, it has been shown that highly branched polymers are formed via step-growth condensation process as a result of the multiple reactive sites present on the benzyl species (i.e., the ortho, meta, and para positions are all reactive[26]).[34−37] At low molecular weights (<5 kDa), PPM is soluble in a wide range of organic solvents but tends to have poor mechanical properties, in part due its low softening temperature (typically less than 80 °C).[38−40] Higher molecular weights can be achieved using metal catalysts,[33,36,38,41] but these polymers are typically insoluble, which challenges processing and subsequent use in applications where structurally robust materials are required.[42] Despite these obstacles and the relative paucity of recent reports on poly(phenylene alkyene)s, PPM and its derivatives exhibit a number of useful properties, including low dielectric constants ($\varepsilon_r = 2.5-2.7$),[43] high thermal stabilities (T_d > 400 °C),[44] high solvent resistance, high hydrophobicity (θ = 87°−90°),[45] and good gas and moisture barrier properties (for example, H_2O permeability typically ranges from 0.6 to 6.0 g mil atm^{-1} 100 in.$^{-2}$ 24 h^{-1} at 25 °C).[28,41,45−48]

In our early optimizations of the GO-catalyzed oxidation of BnOH to benzaldehyde, we observed a polymeric byproduct via NMR spectroscopy when the reaction was performed at high temperatures (>150 °C).[20] Considering that previous reports have shown that H_2SO_4 or other strong acids can polymerize BnOH,[42] we reasoned that this compound would undergo a dehydrative polymerization in the presence of GO as a result of the material's acidity (pH = 4.5 at 1 mg mL^{-1} in water).[49,50] In a preliminary experiment designed to investigate such reactivity, BnOH (3.0 g) was heated with 10 wt % GO (0.3 g) in a sealed vessel to 200 °C for 14 h under vigorous magnetic stirring. Upon cooling to room temperature, the product solidified in the vessel and no visible phase separation of the carbon material was evident. The polymeric portion of the product was found to be soluble in a wide range of organic solvents, including dichloromethane (DCM), *N*,*N*-dimethylformamide (DMF), and tetrahydrofuran (THF).[51] Conversely, the carbon that was used to catalyze the reaction was not soluble in any of these solvents, facilitating its separation from the polymer. Thus, unlike previously described uses of GO for the formation of composites,[12] the polymer and the carbon did not appear to be covalently bound (see below for additional discussion). The water produced as a byproduct was found to phase separate from the solid product and was decanted or removed under vacuum. Furthermore, no other byproducts were observed by NMR spectroscopy of the crude polymer (separated from the carbon by trituration in DCM), which suggested to us that the conversion of the monomer to PPM was quantitative (later verified by mass balance). The molecular weight and polydispersity of the isolated polymer were analyzed by GPC,[52] which revealed a number-average molecular weight (M_n) of 2.3 kDa and a polydispersity index (PDI) of 1.26.[53]

Having demonstrated that GO is capable of catalyzing the polymerization of BnOH, subsequent efforts were directed toward optimizing the reaction with respect to the loading of GO in the starting mixture. At loadings below 7.5 wt %, the as-prepared GO was unable to completely polymerize BnOH; though, above this threshold, monomer conversion was complete.[54] Therefore, in order to maximize formation of the target polymer at lower loadings, 1 wt % H_2SO_4 was added to the reaction mixtures that contained less than 7.5 wt % of GO.[55] As a control, an additive-free sample of PPM was prepared under otherwise identical conditions using only concentrated H_2SO_4 (1 wt %) as the polymerization catalyst. Similar to the product formed using 10 wt % GO, a polymer with a M_n of 2.2 kDa (PDI = 1.18) was obtained. In general, no significant change in M_n was

Table 1. Summary of Poly(phenylene methylene) (PPM) Composites Incorporating Graphene as the Carbon Additive[a]

graphite oxide loading (%)[b]	elastic modulus (E') at 0 °C/MPa[c]	softening point (T_s)/°C[d]	decomposition temp (T_d)/°C[e]	mol wt (M_n)/Da[f]	polydispersity index (PDI)[f]
0.0[g]	40 ± 20[h]	35.43	463.68	2229	1.18
0.01	40 ± 10[h]	38.20	447.01	2316	1.22
0.1	320 ± 20	40.06	472.08	2210	1.27
0.5	310 ± 20	38.31	445.19	2414	1.15
1.0	310 ± 10	36.68	462.55	2310	1.21
5.0	490 ± 20	38.64	444.34	2252	1.12
10.0	915 ± 8	48.27	445.52	2307	1.26
10.0[i]	910 ± 10	47.38	446.83	2218	1.23

[a] Unless otherwise noted, all composites were prepared by reacting 3.0 g of benzyl alcohol with varying amounts of GO (as indicated) and 0.03 g (1 wt %) of H_2SO_4 at 200 °C for 14 h. [b] Prepared via the Hummers method. [c] The elastic (E') and loss moduli (E'') were characterized by dynamic mechanical analysis (DMA). The samples were heated from 0 °C to their softening point (T_s) at a rate of 1 °C min^{-1} while oscillating at a constant amplitude of 50 μm and a frequency of 1 Hz. All measurements were performed in triplicate, and the reported errors represent 1 standard deviation from the mean. [d] Softening points (T_s) were determined by calculating the loss onset of the elastic modulus (E') measured via DMA. [e] Decompostion temperatures (T_d) were determined via thermogravimetric analysis by heating a sample of the composite under nitrogen at a heating rate of 10 °C min^{-1}. [f] Number-average molecular weights (M_n) and polydispersity indices (PDIs) were determined by GPC against poly(styrene) standards after dissolving the polymer in DMF and separating from the carbon additive via filtration. [g] An additive-free PPM was used to compare mechanical, thermal, and molecular weight properties with the GO-derived composites. The polymer was prepared by reacting 3.0 g of benzyl alcohol with 0.03 g (1 wt %) of H_2SO_4 at 200 °C for 14 h. [h] A higher signal-to-noise ratio was observed in the DMA of the additive-free polymer (0 wt % loading) and the composite containing 0.1 wt % loading of GO in the starting mixture. Because of the fragility of these additive-free or low loading samples, and ensuing sample fracture, it was not possible to fully tighten the sample in the dual cantilever clamp; a smoothing algorithm was not applied to these data. [i] Composite prepared by reacting 3.0 g of benzyl alcohol with 10 wt % GO at 200 °C for 14 h. No H_2SO_4 cocatalyst was used.

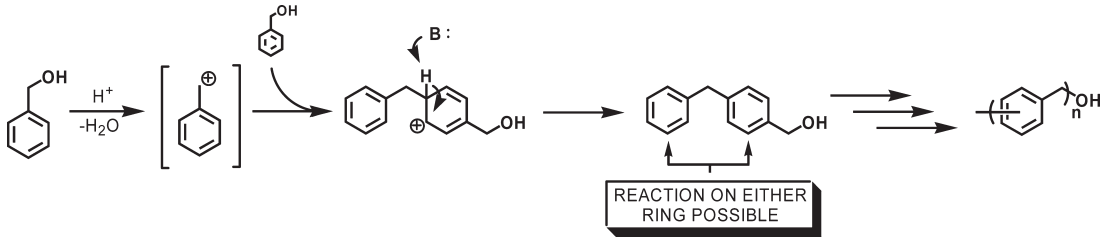

Figure 3. Proposed structure and formation of poly(phenylene methylene) (PPM) synthesized via an acid-catalyzed dehydration process.[33,35,36]

observed as the GO loading or acid content was varied (see Table 1), and the polydispersity indices of the resulting polymers were found to be relatively constant. The observed plateauing of the molecular weight may be due to inactivation of the propagating cation (e.g., termination of the polymerization or chain transfer) at these chain lengths.[56]

In accord with other polymerizations of BnOH, the mechanism of the aforementioned reaction was likely an acid-catalyzed dehydration (see Figure 3).[33,35,36,46,57] The propagating species may react at any of the available positions on the BnOH monomer, with a preference for the available ortho and para positions, and afford a highly branched polymer. For example, the well-defined FT-IR absorbances attributed to the arene moiety in BnOH (1454, 1469 cm^{-1}) were broadened and split to a series of several strong absorbances spanning from 1393 to 1527 cm^{-1} in the corresponding polymer, consistent with a branched structure (see Figures S11 and S12). Likewise, the ^{13}C NMR spectrum of the polymer displayed broad resonances in the arene region (125−141 ppm). The operative acid-catalyzed reaction may be mediated by the carboxylic acid groups present on the edge or surface of GO (see Figure 1)[14,15] or other acidic functional groups on GO's surface.

Having characterized the molecular weight of the polymers obtained using a variety of GO loadings, we next sought to investigate the thermomechanical properties of the polymers and composites. Using dynamic mechanical analysis (DMA), the additive-free polymer was found to exhibit a softening point (T_s) at ∼35 °C.[58] In the PPM composite prepared using 10 wt % GO, the corresponding T_s was measured at 48 °C, indicating that the softening point of the polymer was enhanced upon incorporation into a carbon-filled composite (see Table 1 for T_s values at various GO loadings). Consistent with previous results determined on related poly(*p*-xylylene)s, the additive-free PPM appeared to be thermally stable and exhibited an onset of decomposition (T_d) at 464 °C by thermogravimetric analysis (TGA).[42,45] The onset of decomposition was perturbed only slightly when the additive was incorporated at various GO loadings (i.e., the T_d ranged from 445 to 463 °C; see Table 1). In all of the composites tested, the decompositions occurred in a single event, rather than stepwise, suggesting cooperative effects between the matrix and additive.

Considering that other poly(phenylene alkylene)s (e.g., poly(*p*-xylylene)) have found use as robust structural materials,[45] we next sought to characterize the mechanical properties of PPM and its composites using DMA. Prior to the T_s, the additive-free polymer exhibited an elastic modulus (E') of 40 MPa (see Figure 4); however, the E' increased to 915 MPa upon incorporation of 10 wt % GO in the starting mixture. This result

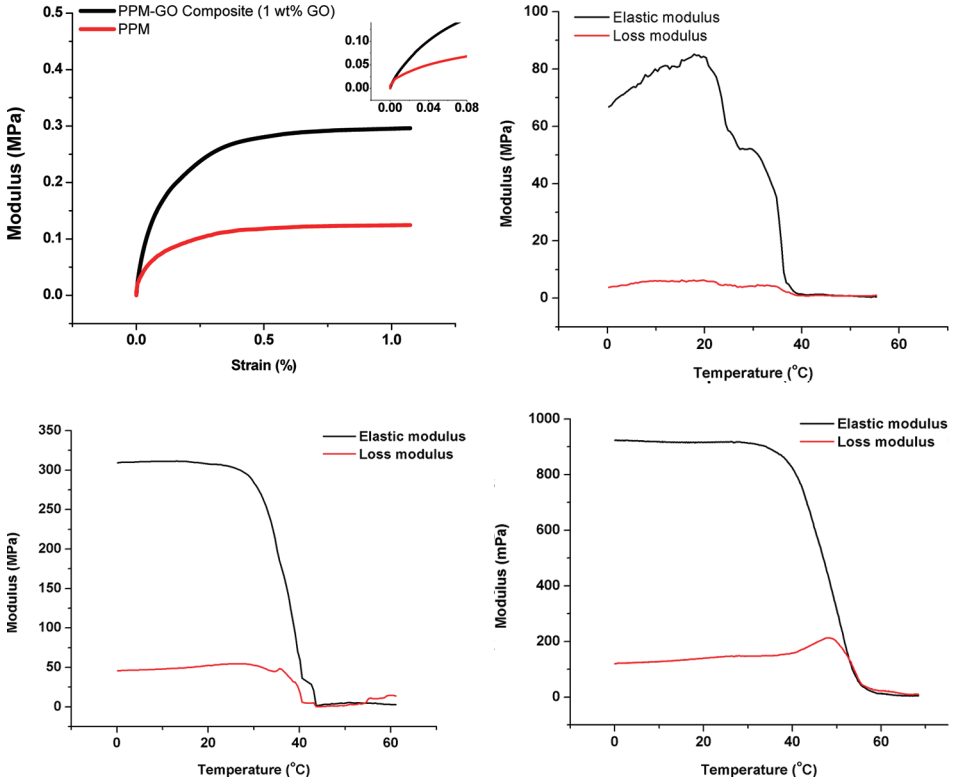

Figure 4. Stress−strain curves of PPM and a PPM−GO composite (1 wt % GO) (top left). Elastic (E') and loss (E'') moduli as a function of temperature for PPM−GO composites at loadings of 0 (top right), 0.1 (bottom left), and 10 wt % GO (bottom right) (single cantilever, 50 μm amplitude, heating rate = 1 °C min^{-1}).

suggested to us that GO not only efficiently catalyzed the polymerization of BnOH but simultaneously functioned as an additive for the enhancement of the stiffness of the resulting polymer.[59,60] While GO and other similar carbon nanomaterials have been used as additives in a range of polymer matrices,[1] to the best of our knowledge this is the first example of GO-derived carbon additives and PPM being integrated into a single composite material.[61]

To understand how varying the GO loading in the starting mixture influenced the mechanical properties of the resulting composites, the carbon content was varied from 0.01 to 10 wt % (relative to the unreacted monomer) (see Table 1). Inclusion of GO at loadings of 0.5 or 1.0 wt % produced composites with nearly the same stiffness as the composite prepared using 0.1 wt % of GO (E' = 310−320 MPa). The E' increased to 490 MPa upon increasing the GO loading to 5.0 wt %. Thus, 1.0 wt % may represent a critical threshold for increasing the modulus of these composites in a linear fashion with respect to the carbon loading (see Figure 5), an observation similar to that seen in other carbon composites.[62]

To determine if the inclusion of GO in the starting mixture was advantageous over the postpolymerization addition of the carbon additive, preformed PPM (M_n = 2.3 kDa), prepared using H_2SO_4 (1 wt %) as the catalyst, was mixed with GO (1 wt %) by stirring the two components at 200 °C for 4 h. Upon cooling, the resulting composite was analyzed by DMA and found to exhibit an elastic modulus of 147 ± 7 MPa (T_s = 34.86 °C); this value is approximately half that of the analogous composite where GO was used as the catalyst to polymerize BnOH (see Table 1). In addition to the practical advantage of eliminating the processing

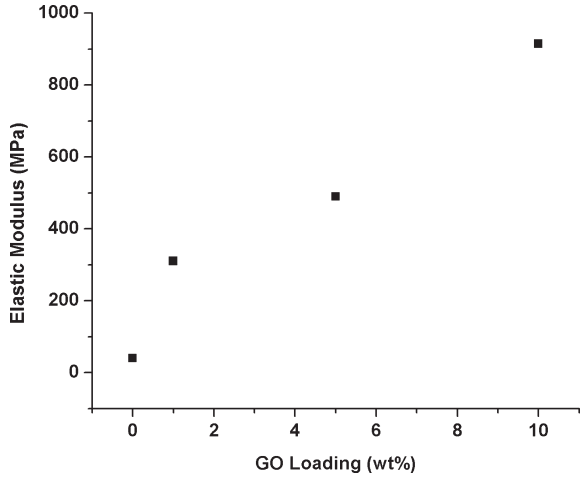

Figure 5. Plot of elastic modulus (MPa) against GO loading in the initial polymerization mixture for various PPM−graphene composites.

step required to blend preformed PPM and GO, these results demonstrated that additional mechanical stiffness may be imparted using a single step approach.

Natural flake graphite and chemically reduced graphene oxide (CReGO) (prepared using hydrazine as a chemical reductant of exfoliated GO according to previously described methods[63]) were also explored as alternate additives to GO to understand how the carbon material's chemical and physical properties (added either prior to or after the polymerization) influence the composites' mechanical and thermal properties.

Table 2. Summary of Poly(phenylene methylene) (PPM) Composites Incorporating Natural Flake Graphite as the Carbon Additive[a]

graphite loading (%)[b]	elastic modulus (E') at 0 °C/MPa[c]	softening point (T_s)/°C[d]	decomposition temp (T_d)/°C[e]	mol wt (M_n)/Da[f]	polydispersity index (PDI)[f]
0.0[g]	30 ± 10[h]	34.31	450.34	2258	1.18
0.01	36 ± 5	35.67	443.89	2241	1.18
0.1	79 ± 7	39.67	451.67	2401	1.27

[a] All composites were prepared by reacting 3.0 g of benzyl alcohol with varying amounts of graphite (as indicated) and 0.03 g (1 wt %) of H_2SO_4 at 200 °C for 14 h. [b] SP-1 natural flake graphite purchase from Bay Carbon, Inc., and used without further purification. [c] The elastic (E') and loss moduli (E'') were characterized by dynamic mechanical analysis (DMA). The samples were heated from 0 °C to their softening point (T_s) at a rate of 1 °C min^{-1} while oscillating at a constant amplitude of 50 μm and a frequency of 1 Hz. All measurements were performed in triplicate, and the reported errors represent 1 standard deviation from the mean. [d] Softening points (T_s) were determined by calculating the loss onset of the elastic modulus (E') measured via DMA. [e] Decompostion temperatures (T_d) were determined via thermogravimetric analysis by heating a sample of the composite under nitrogen at a heating rate of 10 °C min^{-1}. [f] Number-average molecular weights (M_n) and polydispersity indices (PDIs) were determined by GPC against poly(styrene) standards after dissolving the polymer in DMF and separating from the carbon additive via filtration. [g] An additive-free PPM was used to compare mechanical, thermal, and molecular weight properties with the GO-derived composites. The polymer was prepared by reacting 3.0 g of benzyl alcohol with 0.03 g (1 wt %) of H_2SO_4 at 200 °C for 14 h. [h] A higher signal-to-noise ratio was observed in the DMA of the additive-free polymer (0 wt % loading). Because of the fragility of this additive-free sample, and ensuing sample fracture, it was not possible to fully tighten the sample in the dual cantilever clamp; a smoothing algorithm was not applied to these data.

Table 3. Summary of Poly(phenylene methylene) (PPM) Compsites Incorporating Chemically Reduced Graphene Oxide (CReGO) as the Carbon Additive[a]

CReGO loading (%)[b]	elastic modulus (E') at 0 °C/MPa[c]	softening point (T_s)/°C[d]	decomposition temp (T_d)/°C[e]	mol wt (M_n)/Da[f]	polydispersity index (PDI)[f]
0.0[g]	40 ± 20[h]	33.13	450.59	2214	1.18
0.01	180 ± 8	33.04	459.38	2283	1.19
0.1	170 ± 10	32.30	445.49	2246	1.18

[a] All composites were prepared by reacting 3.0 g of benzyl alcohol with varying amounts of chemically reduced graphene oxide (CReGO) (as indicated) and 0.03 g (1 wt %) of H_2SO_4 at 200 °C for 14 h, followed by dissolution of the polymer in DCM and isolation of the carbon product by filtration. [b] Prepared according to previously described methods using hydrazine hydrate ($N_2H_4 \cdot H_2O$) as the chemical reductant.[63] [c] The elastic (E') and loss moduli (E'') were characterized by dynamic mechanical analysis (DMA). The samples were heated from 0 °C to their softening point (T_s) at a rate of 1 °C min^{-1} while oscillating at a constant amplitude of 50 μm and a frequency of 1 Hz. All measurements were performed in triplicate, and the reported errors represent 1 standard deviation from the mean. [d] Softening points (T_s) were determined by calculating the loss onset of the elastic modulus (E') measured via DMA. [e] Decompostion temperatures (T_d) were determined via thermogravimetric analysis by heating a sample of the composite under nitrogen at a heating rate of 10 °C min^{-1}. [f] Number-average molecular weights (M_n) and polydispersity indices (PDIs) were determined by GPC against poly(styrene) standards after dissolving the polymer in DMF and separating from the carbon additive via filtration. [g] An additive-free PPM was used to compare mechanical, thermal, and molecular weight properties with the GO-derived composites. The polymer was prepared by reacting 3.0 g of benzyl alcohol with 0.03 g (1 wt %) of H_2SO_4 at 200 °C for 14 h. [h] A higher signal-to-noise ratio was observed in the DMA of the additive-free polymer (0 wt % loading). Because of the fragility of this additive-free sample, and ensuing sample fracture, it was not possible to fully tighten the sample in the dual cantilever clamp; a smoothing algorithm was not applied to these data.

Using H_2SO_4 as the polymerization catalyst (1 wt %), composites incorporating these carbon materials were prepared using the same *in situ* methods described above (i.e., 3.0 g of BnOH, 0.03 g of concentrated H_2SO_4, 0.0−0.1 wt % carbon, 200 °C, 14 h). The resulting materials exhibited significantly poorer mechanical properties ($E' \leq 180$ MPa) compared to the carbon-filled composites derived from GO (see Tables 2 and 3). Moreover, the T_s of these composites, determined primarily by the identity of the polymer matrix, varied depending on quantity and the composition of the additive (T_s = 32−40 °C). Regardless, in all of the graphite- and CReGO-based composites produced, the carbon additives were visually observed to aggregate and phase separate from the transparent polymer matrix. Such aggregation of these particular carbon additives has been widely observed in other composites[64,65] and often leads to the introduction of stress concentration points, thereby weakening the materials' mechanical integrity.[66] Hence, the relatively poor mechanical performance of these unfunctionalized carbons suggested to us that GO's surface functionality may stabilize the dispersion of the carbon in the polymer matrix.[67]

We also were interested in the fate of the GO and thus sought to characterize the resulting carbon additive and its dispersion in the as-prepared composite. The observation of improved mechanical stiffness in the composites, as compared to the additive-free polymer, suggested to us a good dispersion of the additive in the matrix; however, direct characterization of the structure and morphology of the carbon additive, as well as the polymer matrix, was necessary to support this conclusion. In previous reactions of GO with BnOH, we have found that the carbon product tended to undergo deoxygenation to a graphene-like material, which then underwent restacking to form well-defined, graphite-like aggregates, as confirmed by powder X-ray diffraction (PXRD) analysis and Raman spectroscopy.[68] As reported in our previous work,[68] upon deoxygenation and formation of graphite-like aggregates, a significant increase in the peak position was observed (from $2\theta = 11°$ to $2\theta = 27°$), as well as a concomitant decrease in the I_D/I_G ratio, indicating an overall increase in order

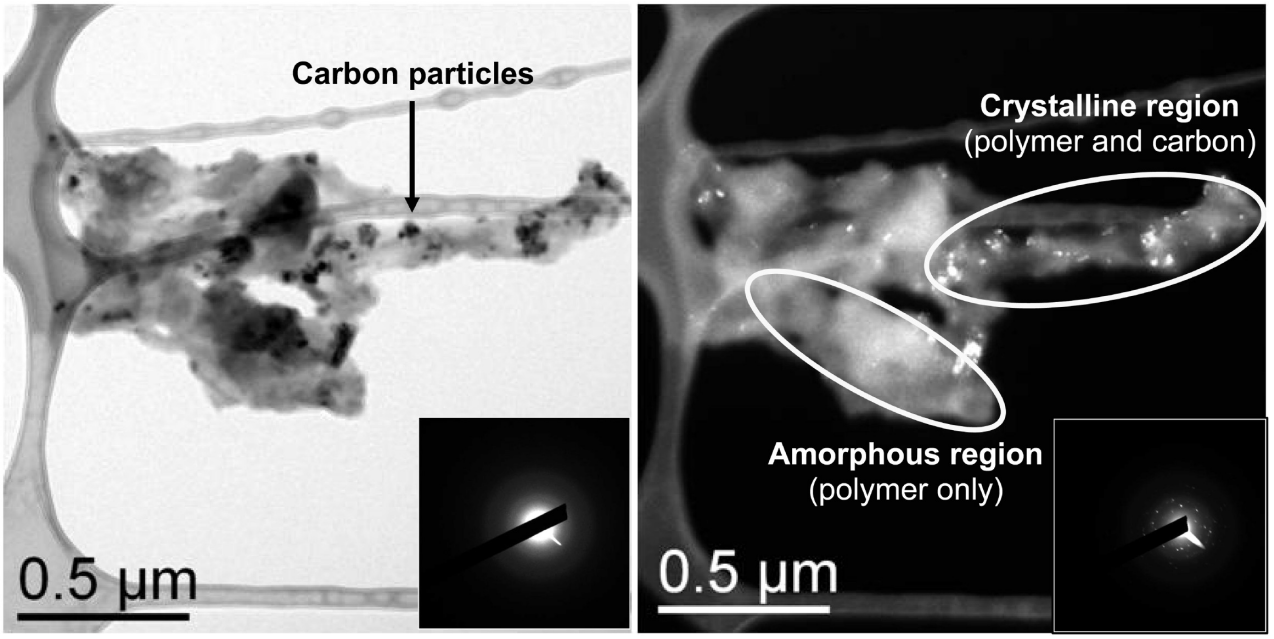

Figure 6. (left) Bright field (BF) and (right) dark field (DF) TEM images of the carbon-filled PPM composite (1 wt % GO loading) showing amorphous and crystalline regions (dark speckles in the BF image and white speckles in the DF image). (left inset) Selected area electron diffraction (SAED) patterns from the amorphous regions and (right inset) the crystalline regions shown in the respective larger images.

within the carbon material. When PXRD was performed on the composite prepared using 1 wt % GO (see Figure S6), a broad reflection centered at $2\theta = 18.7°$, which corresponded to a *d*-spacing of 4.7 Å, was observed. The measured reflection was inconsistent with that observed in graphite ($2\theta = 26.5°$) (see Figure S3).

Surprisingly, analysis of the separated carbon by PXRD did not reveal the expected graphite-like reflection present at $2\theta \approx 26.5°$.[68,69] Rather, a series of broad, low-intensity, ill-defined reflections spanning from $2\theta = 10°-25°$ was observed. These results suggested to us that the carbon, though highly deoxygenated as evidenced by its high conductivity and C:O ratio (see below), did not aggregate into graphite-like particles. Strong interactions between the PPM and the deoxygenated carbon, consistent with intercalation of the polymer into the carbon's interlayer spacing, may have stabilized the dispersion of the carbon in the matrix, both in the melt and in the solid state. The observed disordered structure of the carbon was supported by Raman spectroscopy, which revealed a slight increase in the ratio of the intensities of the D and G bands in the recovered carbon as compared to the GO starting material ($I_D/I_G = 1.23$ and 1.04, respectively) (see Figure S14). Graphite and other highly ordered carbon materials typically exhibit significantly lower I_D/I_G ratios (usually zero, if the graphite is highly ordered; see Figure S13), while high I_D/I_G ratios are characteristic of relatively disordered carbons.[70,71]

To gain further insight into the dispersion of the carbon in the composite containing 1 wt % GO loading, transmission electron microscopy (TEM) was performed on the as-prepared material. Two distinct regions were revealed (see Figure 6): a completely amorphous region, as evidenced by the diffuse ring and lack of spots in the selected area of the electron diffraction (SAED) pattern, as well as a highly crystalline region, as shown by the presence of diffraction spots. The observed amorphous region was consistent with a structure corresponding solely to the polymer material, whereas the crystalline area was consistent with a composite mixture of the carbon additive and PPM.[72] The higher degree of crystallinity seen in the high-resolution transmission electron microscope (HRTEM) image of the as-prepared composite as compared to the pure carbon additive (separated and recovered; see Figure 7) indicated that the polymer cocrystallized around the included carbon additive and formed an interphase region, in accord with observations made on other nanocomposite materials.[1] Within these crystalline regions, the carbon additive was well dispersed, and no phase separation was observed. We surmised that the resulting structure may be responsible for the enhanced mechanical properties previously described. Increased crystallinity within polymers has been shown to enhance mechanical stiffness as well as thermal stability, compared to amorphous samples of the same polymers,[73−75] and as we observed similar enhancements in PPM's mechanical properties, we reasoned that similar effects were operative within the crystalline regions of the composites (see above).[76]

In addition to evaluating the stacking and morphological behavior of the recovered carbon, we also investigated its extent of functionalization. Our previous results have shown that BnOH excels at deoxygenating GO, affording a sparsely functionalized, graphite-like product.[68] To determine if similar products could be observed in the composites produced by treating BnOH with GO under the conditions studied here (1 wt % in the starting mixture), deoxygenation of the GO starting material was evaluated by elemental combustion analysis. The results revealed that the carbon isolated from the composites exhibited a C:O ratio of 12.3:1, as compared to 2.0:1 for the GO starting material. Powder conductivity analysis was also performed on the separated carbon in order to characterize the extent of deoxygenation of the GO starting material. A bulk conductivity (σ) of 801 S m^{-1} was measured, which was significantly higher than the analogous value measured for as-prepared GO ($\sigma = 4.45 \times 10^{-5}$ S m^{-1}).

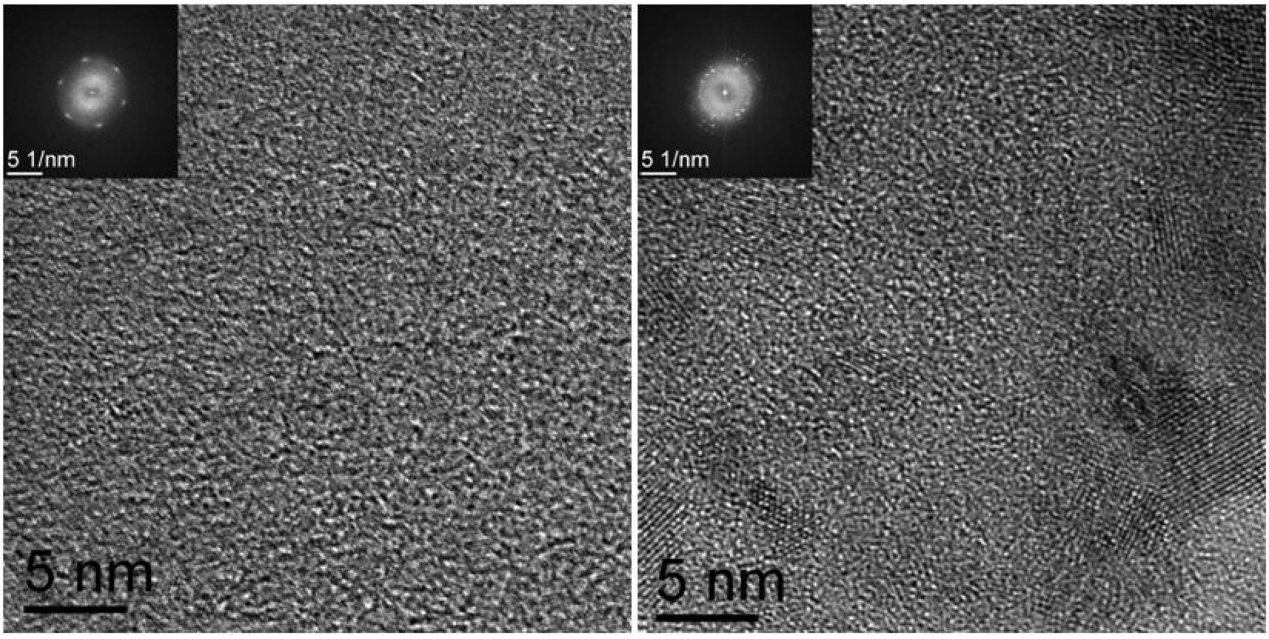

Figure 7. (left) HRTEM images of the recovered carbon additive and (right) the composite, which consisted of carbon additive and polymer. The higher crystallinity present in the composite was confirmed by the fast Fourier transform (FFT) images shown in the insets. The increase in crystallinity is likely a result of cocrystallization of the polymer matrix around the carbon additive particles and formation of an interphase crystalline region within the regions of the composite that included the carbon.

For comparison, graphite, graphene, and reduced graphene oxide exhibit high conductivities (500−2000 S m^{-1}),[63,77−79] similar to the recovered carbon analyzed here, suggesting efficient reformation of the sp^2-hybridized structure found in graphene.[80] Likewise, analysis by FT-IR spectroscopy showed a near complete disappearance of the absorbances associated with the oxygen-containing functionalities present on GO (see Figures S9 and S10).[81] Finally, deoxygenation of the recovered additive was confirmed by TGA, which revealed minimal mass loss prior to 400 °C (heating rate = 10 °C min^{-1} under N_2), in contrast to the GO starting material, which began to decompose immediately upon heating (see Figures S17 and S18). Collectively, the analyses of the recovered carbon indicated that the GO transitioned to a highly deoxygenated and disordered graphene-like material that became trapped in the polymer matrix, allowing it to effectively function as a mechanical reinforcer.[82]

In conclusion, we have shown that GO is capable of catalyzing the dehydrative polymerization of BnOH to PPM in quantitative yield. Moreover, the product obtained at the conclusion of the polymerization reaction incorporated the carbon as a dispersed additive without the need for further processing, indicating this method is a viable one-step approach for forming PPM−carbon composites. While PPM is a structurally compliant material (E' = 40 MPa), reaction of BnOH with as little as 0.1 wt % GO markedly increased the stiffness of the resulting composite (E' = 320 MPa), and the elastic modulus was found to scale with the loading of the carbon. Upon separation, the carbon was found to be significantly deoxygenated, akin to other graphene-like materials, as determined by FT-IR spectroscopy, elemental combustion analysis, and powder conductivity measurements. Moreover, the long range order in the recovered carbon was relatively low and the restacking of carbon layers to form highly ordered graphite-like aggregates was not observed, as determined by PXRD, TEM, and Raman spectroscopy. Taken together, these spectroscopic data indicate that the recovered carbon was mostly disordered and well-dispersed within the polymer matrix. We conclude that this is a direct result of favorable interactions between the additive and the matrix, resulting in a homogeneous dispersion and enhancement of the mechanical properties of the matrix.

Collectively, the results demonstrated herein portend a new method with broad applicability. Specifically, these findings demonstrate that carbon-based catalysts,[24] such as GO, may be used as both a polymerization catalyst and, simultaneously, as an additive in the polymer product, ultimately resulting in polymers with improved properties (mechanical, electrical, barrier, etc.). Such an approach will allow for the formation of robust nanocomposites in a single step using only two reaction components: the monomer and the carbon. As an example of how this method might be realized for the preparation of other composites, other dehydration polymerizations are strong candidates for GO-mediated acid catalysis, and many of these carbon-filled structural composites have found widespread use.[83−85] In a broader perspective, the promise of GO and other graphene-based materials now extends beyond the utilization and exploitation of their remarkable electronic and mechanical properties and poises them to address synthetic issues at the frontier of polymer chemistry, particularly for offering metal-free methodologies and for facilitating the synthesis of polymer−carbon composites.

■ ASSOCIATED CONTENT

Supporting Information. Detailed experimental procedures and additional characterization details. This material is available free of charge via the Internet at http://pubs.acs.org.

AUTHOR INFORMATION

Corresponding Author
*E-mail: bielawski@cm.utexas.edu.

ACKNOWLEDGMENT

We gratefully acknowledge support for this work provided by the National Science Foundation (Grant DMR-0907324) and the Robert A. Welch Foundation (Grant F-1621).

REFERENCES

(1) Potts, J. R.; Dreyer, D. R.; Bielawski, C. W.; Ruoff, R. S. *Polymer* **2011**, *52*, 5–25.
(2) Balazs, A. C.; Emrick, T.; Russell, T. P. *Science* **2006**, *314*, 1107–1110.
(3) Kumar, S.; Lively, B.; Liu, T.; Sun, L.; Tangpong, A.; Zhong, W.-H. *Macromol. Mater. Eng.* **2011**, *296*, 151–158.
(4) Kim, H.; Macosko, C. W. *Polymer* **2009**, *50*, 3797–3809.
(5) Choi, E.-Y.; Han, T. H.; Hong, J.; Kim, J. E.; Lee, S. H.; Kim, H. W.; Kim, S. O. *J. Mater. Chem.* **2010**, *20*, 1907–1912.
(6) Feng, R.; Guan, G.; Zhou, W.; Li, C.; Zhang, D.; Xiao, Y. *J. Mater. Chem.* **2011**, *21*, 3931–3939.
(7) Wang, D.-W.; Li, F.; Zhao, J.; Ren, W.; Chen, Z.-G.; Tan, J.; Wu, Z.-S.; Gentle, I.; Lu, G. Q.; Cheng, H.-M. *ACS Nano* **2009**, *3*, 1745–1752.
(8) Xu, Z.; Gao, C. *Macromolecules* **2010**, *43*, 6716–6723.
(9) Viswanathan, G.; Chakrapani, N.; Yang, H.; Wei, B.; Chung, H.; Cho, K.; Ryu, C. Y.; Ajayan, P. M. *J. Am. Chem. Soc.* **2003**, *125*, 9258–9259.
(10) Kong, H.; Gao, C.; Yan, D. *J. Am. Chem. Soc.* **2004**, *126*, 412–413.
(11) Wang, X.; Hu, Y.; Song, L.; Yang, H.; Xing, W.; Lu, H. *J. Mater. Chem.* **2011**, *21*, 4222–4227.
(12) Lee, S. H.; Dreyer, D. R.; An, J.; Velamakanni, A.; Piner, R. D.; Park, S.; Zhu, Y.; Kim, S. O.; Bielawski, C. W.; Ruoff, R. S. *Macromol. Rapid Commun.* **2010**, *31*, 281–288.
(13) Zhang, B.; Chen, Y.; Xu, L.; Zeng, L.; He, Y.; Kang, E.-T.; Zhang, J. *J. Polym. Sci., Part A: Polym. Chem.* **2011**, *49*, 2043–2050.
(14) Dreyer, D. R.; Park, S.; Bielawski, C. W.; Ruoff, R. S. *Chem. Soc. Rev.* **2010**, *39*, 228–240.
(15) Lerf, A.; He, H.; Forster, M.; Klinowski, J. *J. Phys. Chem. B* **1998**, *102*, 4477–4482.
(16) Lee, S. H.; Kim, H. W.; Hwang, J. O.; Lee, W. J.; Kwon, J.; Bielawski, C. W.; Ruoff, R. S.; Kim, S. O. *Angew. Chem., Int. Ed.* **2010**, *49*, 10084–10088.
(17) Gao, X.; Jang, J.; Nagase, S. *J. Phys. Chem. C* **2010**, *114*, 832–842.
(18) Jung, I.; Field, D. A.; Clark, N. J.; Zhu, Y.; Yang, D.; Piner, R. D.; Stankovich, S.; Dikin, D. A.; Geisler, H.; Ventrice, C. A., Jr.; Ruoff, R. S. *J. Phys. Chem. C* **2009**, *113*, 18480–18486.
(19) Acik, M.; Mattevi, C.; Gong, C.; Lee, G.; Cho, K.; Chhowalla, M.; Chabal, Y. J. *ACS Nano* **2010**, *4*, 5861–5868.
(20) Dreyer, D. R.; Jia, H.-P.; Bielawski, C. W. *Angew. Chem., Int. Ed.* **2010**, *49*, 6813–6816.
(21) Jia, H.-P.; Dreyer, D. R.; Bielawski, C. W. *Adv. Synth. Catal.* **2011**, *353*, 528–532.
(22) Jia, H.-P.; Dreyer, D. R.; Bielawski, C. W. *Tetrahedron* **2011**, *67*, 4431–4434.
(23) Pyun, J. *Angew. Chem., Int. Ed.* **2011**, *50*, 46–48.
(24) Dreyer, D. R.; Bielawski, C. W. *Chem. Sci.* **2011**, *2*, 1233–1240.
(25) Xu, L. Q.; Liu, Y. L.; Neoh, K.-G.; Kang, E.-T.; Fu, G. D. *Macromol. Rapid Commun.* **2011**, *32*, 684–688.
(26) Lenz, R. W. In *Organic Chemistry of Synthetic High Polymers*; Interscience Publishers: New York, 1967; pp 228−231.
(27) Gibbons, R. A.; Gibbons, M. N.; Wolfrom, M. L. *J. Am. Chem. Soc.* **1955**, *77*, 6374.
(28) Steiger, D.; Tervoort, T.; Weder, C.; Smith, P. *Macromol. Rapid Commun.* **2000**, *21*, 405–422.
(29) Cannizzaro, S. *Liebigs Ann. Chem.* **1854**, *90*, 252–254.
(30) Cannizzaro, S. *Liebigs Ann. Chem.* **1854**, *92*, 113–117.
(31) Friedel, C.; Crafts, J. M. *Bull. Soc. Chim.* **1885**, 43.
(32) M'Hiri, T.; Catusse, C.; Catusse, R.; Dubry, J. L. J. *React. Kinet. Catal. Lett.* **1983**, *22*, 425–428.
(33) Parker, D. B. V.; Davies, W. G.; South, K. D. *J. Chem. Soc. B* **1967**, 471–477.
(34) Flory, P. J. *J. Am. Chem. Soc.* **1952**, *74*, 2718–2723.
(35) Montaudo, G.; Finocchiaro, P.; Caccamese, S.; Bottino, F. *J. Polym. Sci., Part A: Polym. Chem.* **1970**, *8*, 2475–2490.
(36) Valentine, L.; Winter, R. W. *J. Chem. Soc.* **1956**, 4768–4779.
(37) Jacobson, R. A. *J. Am. Chem. Soc.* **1932**, *54*, 1513–1518.
(38) Shriner, R. L.; Berger, A. *J. Org. Chem.* **1941**, *06*, 305–318.
(39) Olazar, M.; Bilbao, J.; Aguayo, A. T.; Romero, A. *Ind. Eng. Chem. Res.* **1987**, *26*, 1956–1960.
(40) Bilbao, J.; Olazar, M.; Arandes, J. M.; Romero, A. *Ind. Eng. Chem. Res.* **1987**, *26*, 1960–1965.
(41) Bilbao, J.; Olazar, M.; Romero, A.; Arandes, J. M. *Ind. Eng. Chem. Res.* **1987**, *26*, 1297–1304.
(42) Banks, R. E.; François, P.-Y.; Preston, P. N. *Polymer* **1992**, *33*, 3974–3975.
(43) Senkevich, J. J.; Desu, S. B. *Appl. Phys. A: Mater. Sci. Process.* **2000**, *70*, 541–546.
(44) Schaefgen, J. R. *J. Polym. Sci.* **1959**, *41*, 133–141.
(45) Gorham, W. F. *J. Polym. Sci., Part A: Polym. Chem.* **1966**, *4*, 3027–3039.
(46) Gunes, D.; Yagci, Y.; Bicak, N. *Macromolecules* **2010**, *43*, 7993–7997.
(47) Szwarc, M. *Polym. Eng. Sci.* **1976**, *16*, 473–479.
(48) Bilbao, J.; Olazar, M.; Arandes, J. M.; Romero, A. *Chem. Eng. Commun.* **1989**, *75*, 121–134.
(49) Szabó, T.; Tombácz, E.; Illés, E.; Dékány, I. *Carbon* **2006**, *44*, 537–545.
(50) Szabó, T.; Berkesi, O.; Forgó, P.; Josepovits, K.; Sanakis, Y.; Petridis, D.; Dékány, I. *Chem. Mater.* **2006**, *18*, 2740–2749.
(51) Upon separation of the polymer from the additive via trituration in DCM, we also found that PPM exhibited remarkable photophysical properties. The separated PPM displayed an absorption maximum (λ_{abs}) of 222 nm (see Figure S1) in the solution state (THF) with an extinction coefficient of 79.2 mL mg^{-1} cm^{-1}. The polymer was also analyzed by fluorimetry (see Figure S2) and an emission maximum (λ_{em}) of 411 nm was measured (λ_{ex} = 259 nm), with a quantum efficiency (ϕ) of 0.58 against quinine sulfate using previously established methods (see: Eastman, J. W. *Photochem. Photobiol.* **1967**, *6*, 55–72). PPM formed in the absence of GO, using only H_2SO_4 as the polymerization catalyst, exhibited identical photophysical properties.
(52) It has been shown that branched and hyperbranched polymers elute at artificially long times, relative to linear polymers, due to their unique interactions with the porous columns used in gel permeation chromatography (see: Podzimek, S.; Vlcek, T.; Johann, C. *J. Appl. Polym. Sci.* **2001**, *81*, 1588–1594). Therefore, the polymers were also characterized using a GPC equipped with a triple detector (right angle light scattering, intrinsic viscosity, and refractive index) in order to determine the polymer's absolute molecular weight. A molecular weight of 5.2 kDa (PDI = 1.41) was measured, indicating that using a GPC equipped with a simple RI detector provided a good approximation of PPM's molecular weight and size distribution.
(53) Podzimek, S.; Vlcek, T.; Johann, C. *J. Appl. Polym. Sci.* **2001**, *81*, 1588–1594.
(54) At loadings below 7.5 wt % GO, conversion of BnOH to PPM remained quantitative in the absence of H_2SO_4, but the M_n's of the polymeric products were appreciably lower. At 2.5 wt % GO, a M_n of 1.3 kDa (PDI = 1.10) was measured, while at 5.0 wt % GO a M_n of 1.9 kDa (PDI = 1.12) was measured. These composite mixtures did not solidify at room temperature and were not characterized further.
(55) When benzyl chloride was substituted for benzyl alcohol and subjected to reflux in the presence of GO (1 wt %) in an open vessel attached to a condenser, it was found that additional acid was not necessary to attain polymers of similar molecular weight (M_n = 2.3 kDa;

PDI = 2.13). In fact, lower molecular weights were observed when additional concentrated H_2SO_4 (1 wt %) was added (M_n = 1.0 kDa; PDI = 1.81), suggesting GO may exhibit Lewis acidity in addition to Brønsted acidity.

(56) Endres, G. F.; Overberger, C. G. *J. Am. Chem. Soc.* **1955**, *77*, 2201–2205.

(57) Though we have found that GO can oxidize benzylic methylenes to the corresponding ketones (see: Jia, H.-P.; Dreyer, D. R.; Bielawski, C. W. *Tetrahedron* **2011**, *67*, 4431−4434), the polymeric analogue of this product was not observed in any of our PPM products by ^1H or ^{13}C NMR spectroscopy or FT-IR spectroscopy, consistent with PPM's previously reported stability to oxidizing agents (see: Shriner, R. L.; Berger, A. *J. Org. Chem.* **1941**, *06*, 305−318).

(58) No maximum was observed in either the loss modulus (E'') or the tan δ upon heating beyond the softening point, and no rubbery regime was observed as the sample yielded rapidly upon exceeding the softening point. Thus, this transition is not believed to be a glass transition (T_g) or a true melting point (T_m).

(59) Tensile stress−strain curves performed on both the additive-free polymer and a 1 wt % composite showed nonlinearity throughout the strain profile.

(60) Tensile stress−strain measurements have been performed on poly(*p*-xylylenes) (see: Gorham, W. F. *J. Polym. Sci., Part A: Polym. Chem.* **1966**, *4*, 3027–3039), and Young's modulus values ranging from 1.2 to 3.2 GPa were reported, depending on the arene's substitution (note: poly(phenylene methylene) was not tested, and we are unaware of any mechanical data reported on this polymer). However, plots of these stress−strain curves were not provided, and thus their linearity/nonlinearity could not be evaluated for comparison.

(61) Incorporation of the additive was found to increase the hydrophilicity of PPM upon inclusion: the equilibrium water contact angle changed from 67° in pure PPM to 91° in the PPM−GO composite (1 wt % GO) (see Figures S25 and S26), likely as a result of graphene's high hydrophobicity.

(62) Sandler, J.; Werner, P.; Shaffer, M. S. P.; Demchuk, V.; Altstädt, V.; Windle, A. H. *Composites, Part A* **2002**, *33*, 1033–1039.

(63) Stankovich, S.; Dikin, D. A.; Piner, R. D.; Kohlhaas, K. A.; Kleinhammes, A.; Jia, Y.; Wu, Y.; Nguyen, S. T.; Ruoff, R. S. *Carbon* **2007**, *45*, 1558–1565.

(64) Chen, G.; Zhao, W. In *Nano- and Biocomposites*; Lau, A. K.-T., Hussain, F., Lafdi, K., Eds.; CRC Press: New York, 2010; pp 79−106.

(65) The graphite's structure was found to be unchanged during the polymerization process, as confirmed by PXRD and Raman spectroscopic analysis of the separated carbon material.

(66) Lim, J. K.; Kim, Y. J. *J. Mech. Sci. Technol.* **2001**, *15*, 1616–1622.

(67) Medhekar, N. V.; Ramasubramaniam, A.; Ruoff, R. S.; Shenoy, V. B. *ACS Nano* **2010**, *4*, 2300–2306.

(68) Dreyer, D. R.; Murali, S.; Zhu, Y.; Ruoff, R. S.; Bielawski, C. W. *J. Mater. Chem.* **2011**, *21*, 3443–3447.

(69) Talyzin, A. V.; Szabó, T.; Dékány, I.; Langenhorst, F.; Sokolov, P. S.; Solozhenko, V. L. *J. Phys. Chem. C* **2009**, *113*, 11279–11284.

(70) Ferrari, A. C. *Solid State Commun.* **2007**, *143*, 47–57.

(71) Kudin, K. N.; Ozbas, B.; Schniepp, H. C.; Prud'homme, R. K.; Aksay, I. A.; Car, R. *Nano Lett.* **2008**, *8*, 36–41.

(72) Though analysis of pure PPM by PXRD revealed a broad reflection, indicative of some crystallinity within the additive-free bulk polymer, no crystallinity was observable by TEM, suggesting the degree of crystallinity in the pure polymer was much lower than the composite (1 wt % GO in the starting mixture).

(73) Wang, Y.-J.; Pan, Y.; Kim, D. *Polym. Int.* **2007**, *56*, 381–388.

(74) Sikdar, D.; Katti, D. R.; Katti, K. S.; Bhowmik, R. *Int. J. Multiscale Comp. Eng.* **2010**, *8*, 561–584.

(75) Talbott, M. F.; Springer, G. S.; Berglund, L. A. *J. Compos. Mater.* **1987**, *21*, 1056–1081.

(76) To investigate the extent of the observed crystallinity in the bulk material, analysis of the additive-free polymer as well as the composites prepared using a 1 or 10 wt % loading of GO was performed using differential scanning calorimetry (DSC). These calorimetric analyses revealed transitions only at the materials' softening temperatures (T_s = 35−47 °C). No other discernible exothermic transitions were observed. The lack of a distinguishable melting point above the T_s suggested to us that the bulk of the polymer remained amorphous in the composite and that the crystallinity observed by HRTEM comprised only a very small amount of the polymer within the composite material, consistent with previous observations on the extent of interphase formation in mechanically robust composites (see: Cheeseman, B. A.; Santare, M. H. *J. Compos. Mater.* **2002**, *36*, 553−569).

(77) Buerschaper, R. A. *J. Appl. Phys.* **1944**, *15*, 452–454.

(78) Skrypnyk, Y. V.; Loktev, V. M. *Phys. Rev. B* **2010**, *82*, 085436.

(79) Park, S.; An, J.; Potts, J. R.; Velamakanni, A.; Murali, S.; Ruoff, R. S. *Carbon* **2011**, *49*, 3019–3023.

(80) Zhu, Y.; Stoller, M. D.; Cai, W.; Velamakanni, A.; Piner, R. D.; Chen, D.; Ruoff, R. S. *ACS Nano* **2010**, *4*, 1227–1233.

(81) Though highly disordered, analysis of the carbons using nitrogen adsorption−desorption isotherms, according to the BET method, revealed a low specific area for both GO and the recovered product (2.3 and 9.4 $m^2\ g^{-1}$, respectively).

(82) McNally, T.; Pötschke, P.; Halley, P.; Murphy, M.; Martin, D.; Bell, S. E. J.; Brennan, G. P.; Bein, D.; Lemoine, P.; Quinn, J. P. *Polymer* **2005**, *46*, 8222–8232.

(83) Tortet, L.; Gavarri, J. R.; Nihoul, G.; Dianoux, A. J. *Solid State Ionics* **1997**, *97*, 253–256.

(84) Liu, Y.-L.; Yu, C.-H.; Lai, J.-Y. *J. Membr. Sci.* **2008**, *315*, 106–115.

(85) Huang, S.-H.; Hung, W.-S.; Liaw, D.-J.; Lo, C.-H.; Chao, W.-C.; Hu, C.-C.; Li, C.-L.; Lee, K.-R.; Lai, J.-Y. *Sep. Purif. Technol.* **2010**, *72*, 40–47.